Role of the IgE variable heavy chain in FcεRIα and superantigen binding in allergy and immunotherapy

Wai-Heng Lua, BSc,[a]* Chinh Tran-To Su, PhD,[a]* Joshua Yi Yeo, Dip,[a] Jun-Jie Poh, Dip,[a] Wei-Li Ling, BSc,[a] Ser-Xian Phua, Dip,[a] and Samuel Ken-En Gan, PhD[a,b] *Singapore*

Background: Variable heavy chain (VH) family frameworks (FWRs) have been reported to affect antibody receptor and superantigen binding; however, such effects in IgE remain largely unknown. Given that VH family biases have been previously reported in IgE of certain allergies, there is a need to investigate this phenomenon for biotechnological and therapeutic purposes.

Objective: We sought to investigate the effects of VH families on IgE interaction with FcεRIα, anti-IgE omalizumab, antigen, and superantigen protein A (spA) by using the pertuzumab and trastuzumab IgE models.

Methods: Pertuzumab VH1–VH7 family variants of IgE with the same complementarity-determining regions were investigated with regard to their binding interactions to FcεRIα, Her2, omalizumab, and spA. Notable FcεRIα-IgE observations were cross-checked against appropriate trastuzumab IgE VH variants. Computational structural modeling and simulations were also performed for insight into the mechanism of interactions with various VH FWRs.

Results: The pertuzumab VH5 IgE variant, but not the trastuzumab VH5 IgE, was found to interact with FcεRIα significantly longer than the respective VH family variants within each model antibody. No significant differences in interaction were found between IgE and omalizumab for the pertuzumab VH variants. Although trastuzumab VH3 interacted with spA, none of our pertuzumab VH variants, including VH3, associated with spA.

Conclusion: We found unexpected varying allosteric communications caused by the VH family FWRs to the FcεRIα-, Her2-, and spA-binding regions of pertuzumab IgE, with implications for use of IgE/anti-IgE therapeutics to treat allergy and IgE therapeutics in allergo-oncology. (J Allergy Clin Immunol 2019;■■■:■■■-■■■.)

Key words: *Allergy, IgE, antibodies, variable heavy chain families, allostery, Fc receptor binding, superantigen binding*

Abbreviations used

CDR:	Complementarity-determining region
C-region:	Constant region
FWR:	Framework
ka:	Association rate constant
KD:	Equilibrium dissociation constant
kd:	Dissociation rate constant
PDB:	Protein Data Bank
spA:	Protein A
VH:	Variable heavy chain
V-region:	Variable region

IgE is the main immunoglobulin isotype associated with type 1 hypersensitivity and mast cell/basophil activation.[1,2] The cellular activation typically results from multivalent allergen binding[1] to the variable regions (V-regions) of FcεRIα-bound IgE, but recent evidence suggest the possibility of mast cell receptor activation with IgE alone, without the presence of a known antigen.[3,4] As such, current intervention strategies for allergy activation in using an anti-IgE antibody (omalizumab) to target and deplete the free IgE indirectly reduce mast cell FcεRI expression and activity.[5-7] Such anti-IgE strategies can also disrupt preformed FcεRIα-IgE complexes, although only at very high concentrations of omalizumab, both *in vitro* and *ex vivo*.[8,9]

Within IgE V-regions, there are reports of overrepresentation of specific variable heavy chain (VH) framework (FMR) families in the IgE population, such as VH1 in patients with peanut allergy[10] and VH5 in asthmatic patients[11,12] and patients with allergic rhinitis.[13] However, these studies[10-14] were typically performed on mucosal tissues, whereas studies on PBMCs do not show such biases.[15-19] The reason for such discrepancies was suggested to be due to the presence of specific antigens or superantigens in these tissues, noting that unlike mucosal surfaces, blood is typically sterile and free from microorganisms.

Superantigens typically bind indiscriminately to antibodies and have been industrially exploited for antibody purification methods.[20] They are reported to interact with specific VH FWRs (eg, protein A [spA] to some VH3 FWRs),[21-24] but because not all the same VH FWRs bind to such superantigens, there is no reason to believe that VH FWRs are the sole factors in superantigen binding. As a possible mechanism for superantigen activation of FcεRIα-bound IgE, recent investigations on antibodies have demonstrated that antigen binding at antibody V-regions can elicit structural changes that facilitate cell signaling[25] and that even VH families can elicit distal effects on antibody constant regions (C-regions) for IgGs[26-29] and IgA.[30] This allosteric effect was also shown when the changing of antibody C-regions affected antigen binding.[31]

To investigate the effects of different VH family FWRs on FcεRIα and superantigen binding, as well as for anti-IgE

From [a]the Bioinformatics Institute and [b]the p53 Laboratory, Agency for Science, Technology and Research (A*STAR).

*These authors contributed equally to this work.

Supported by A*STAR Industry Alignment Fund (IAF) grant IAF111149 and institute core funds.

Disclosure of potential conflict of interest: The authors declare that they have no relevant conflicts of interest.

Received for publication October 25, 2018; revised March 25, 2019; accepted for publication March 29, 2019.

Corresponding author: Samuel Ken-En Gan, PhD, Bioinformatics Institute, A*STAR, 30 Biopolis St, #07-01 Matrix, Singapore 138671. E-mail: samuelg@bii.a-star.edu.sg.

0091-6749

© 2019 Elsevier Ltd. All rights reserved.

https://doi.org/10.1016/j.jaci.2019.03.028

therapeutics, we investigated 7 VH families using pertuzumab antibody as a model for grafting onto the IgE C-region[31] and measured interactions with FcεRIα, superantigen spA, anti-IgE (omalizumab), and Her2 using biolayer interferometry. Trastuzumab VH family variants were also investigated as a cross-check to any possible VH FWR effects found on pertuzumab.

METHODS

Cloning of antibodies

Complementarity-determining regions (CDRs) of pertuzumab and trastuzumab VHs were grafted onto the various germline VH families representative of VH1 to VH7, as previously described (Fig 1).[32] The VH families were joined to the IgE C-region, as previously performed.[31,33] Plasmids were transformed into homemade competent DH5α bacteria, as previously described,[34] and extracted by using our in-house extraction kits.[35] To allow us to minimize differences for future more in-depth investigations, trastuzumab was selected as a cross-checking model because the trastuzumab-pertuzumab pair shared high sequence similarity, had the same VH3 FWR, were both specific against Her2, and were produced by the same company (see Fig E1 in this article's Online Repository at www.jacionline.org).

Production and purification of FcεRIα

The extracellular FcεRIα portion of the high-affinity IgE receptor (accession no: NP_001992.1, amino acids 1-201) with a 10× C-terminal HIS tag was cloned and expressed, as previously described for FcγIIA.[32] The secreted protein was purified from the supernatants of transfected cells by using affinity chromatography with the Cobalt column (catalog no. 28953766; GE Healthcare, Chicago, Ill), followed by gel-filtration fractionation with the Superdex 200-pg 16/600 column (GE Healthcare). Peaks corresponding to 25 kDa were kept and further concentrated by using a 10-kDa Amicon Ultra protein concentrator (catalog no. ACS501024; Merck-Millipore, Burlington, Mass).

Production and purification of antibodies

Pertuzumab and trastuzumab VH1–VH7 IgE variants were produced by means of cotransfection, as previously performed.[30-32,36] Affinity purification was carried out with the Protein L column, followed by size exclusion chromatography fractionation with the Superdex 200-pg 16/600 column (GE Healthcare) to extract monomeric fractions, which were further concentrated by using a 100-kDa Amicon Ultra protein concentrator (catalog no. ACS510024; Merck-Millipore). Size exclusion chromatography figures were generated from Unicorn 6.0 software (GE Healthcare), with lines thickened for visibility by using GIMP 2.9.4 software.

Biolayer interferometric studies

Measurements of the association and dissociation rates of the antibodies to spA were carried out by means of direct binding of antibodies at concentrations from 100 to 6.25 nmol/L by using Protein A biosensors (catalog no. 18-5010; ForteBio, Fremont, Calif).

Measurements of pertuzumab IgE variants to Her2 were carried out by loading Her2 on an Ni-NTA biosensor, followed by IgE binding, as previously described.[30-32,36,37] Measurements toward FcεRIα were performed in the same manner, as previously described.[32] Measurements of association and dissociation rates of omalizumab to pertuzumab variants were performed with omalizumab preloaded to Anti-hIgG-Fc Capture biosensors (catalog no. 18-5060; ForteBio), followed by exposure to recombinant pertuzumab antibodies in concentrations ranging from 200 to 12.5 nmol/L.

All measurements were performed with serial dilutions by using the 1× kinetic buffer (catalog no. 18-1092; ForteBio) on the Octet RED96 system (catalog no. 30-5051; ForteBio). All kinetic readings (equilibrium dissociation constant [KD], association constant [ka], and dissociation constant [kd]) were generated by using Octet data analysis software 10.0, and graphs of the representative set from 3 independent repeats were plotted by using Microsoft Excel 2010 (Microsoft, Redmond, Wash). KD and errors for KD, ka, and kd were calculated automatically by the software, where KD = kd/ka.

Computational binding analyses of spA and trastuzumab/pertuzumab VH regions

Binding simulations of spA (Protein Data Bank [PDB]: 1DEE_chain G) and VH regions of trastuzumab (PDB: 1N8Z_chainB) and pertuzumab (PDB: 1S78_chainD) were performed by using the HADDOCK2.2 Web server.[38] As reported in Graille et al,[21] interfacial residues of spA (Q19, G22, F23, Q25, S26, D29, D30, Q33, N36, E40, and L44) and VH (G15, S17, R19, K58, Y60, K65, G66, R67, T69, S71, Q82, N84, and S85) were used as interacting residues for docking.

To first evaluate HADDOCK 2.2 reproducibility for our purposes, we used the structure of IgM^{Fab} and the spA complex (PDB: 1DEE) for initial docking. Individual structures of IgM^{Fab} and spA were separated and redocked at the interface. Because HADDOCK was able to reasonably reproduce the original binding mode of spA and IgM^{VH} (at the highest ranked cluster and the highest score), we proceeded with the subsequent docking of spA to the 2 VH variants. To estimate the lower bound docking scores of the nonbinder, we performed docking of spA to the light chain of the IgM^{Fab} (1DEE_chain A) and used it as a negative reference result (because spA only binds to the VH region).[21,39,40]

The 4 best-docked structures of each antibody/spA complex that resulted in similar binding modes (as aligned to the reference structure 1DEE) were retrieved and minimized by using GROMACS 4.6.7.[41] Binding energies were estimated by using the "gmmpbsa" package[42,43] for all minimized structures.

Structural modeling of full-length unbound trastuzumab and pertuzumab IgE variants

Models of full-length trastuzumab and pertuzumab IgEs were constructed by using scaffolds of a full-length unbound IgE bent structure (kindly provided by Professor Carmay Lim, Academia Sinica, Taipei, Taiwan). From this scaffold template, we performed computational mutagenesis (with SCWRL4[44]) for the light chains (ie, trastuzumab using PDB: 1N8Z_chainA and pertuzumab using PDB: 1S78_chainC) and the VH regions of variants VH1–VH7. We performed energy minimization and equilibration (1 ns) in the explicit solvent with sequential NVT (constant Number of particles, Volume, and Temperature) and NPT (constant Number of particles, Pressure, and Temperature) ensembles using GROMACS 4.6.7[41] for all model structures.

Allosteric communication between the VH and FcεRIα/omalizumab-binding regions

Allosteric communications between the Fab and Fc regions were quantified by using the AlloSigMA server,[45] which had previously successfully quantified allosteric communications in various benchmarked allosteric-involved functional proteins.[45,46] Allosteric communications were estimated based on residual responses to perturbations at the site of interest. To detect the underlying allosteric mechanism that led to different FcεRIα-binding abilities among the various VH variants, we focused on communications between the VH region and the FcεRIα-binding site in the Fc region.

We first initiated perturbations at the different VH FWR regions that distinguished the VH1–VH7 variants from the original VH3 sequence (underlined residues are shown in Fig 1; ie, assigning them as the "down" mutation in the AlloSigMA server[45] to simulate the alanine mutagenesis at these regions), followed by calculating the allosteric responses at the FcεRIα-binding site ($\Delta g_{FcεRIα}$) or at the omalizumab-binding site ($\Delta g_{Omalizumab}$). The FcεRIα-binding site involved residues R334 and D362 of chain A and residue P426 of chain C in the Fc region, and the omalizumab-binding site involved residues S375, R376, S378, K380, E414, Q417, R419, R427, and M430 of

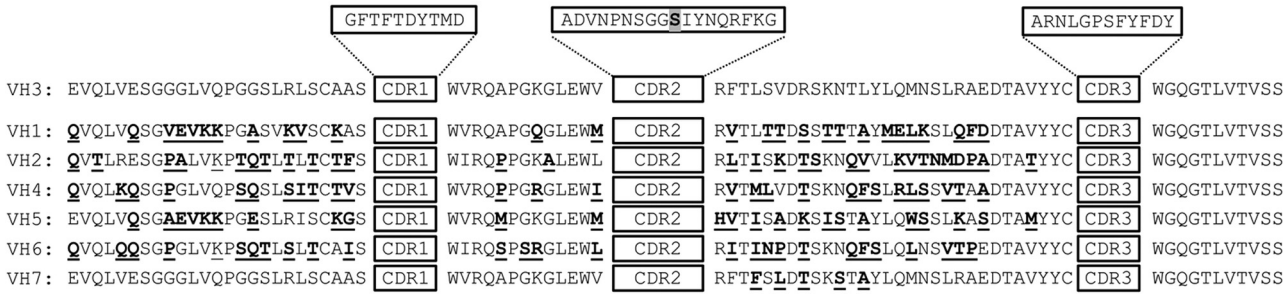

FIG 1. Sequences of the pertuzumab IgE variants VH1 to VH7. Different FWR residues are shown in boldface and underlined with reference to VH3. All variants shared the same CDR sequences shown in the *boxes*. The S58 residue, which played a role in disrupting spA binding, is shaded in the CDR2 sequence. The same manner of grafting was also used for trastuzumab VH family variants.[32]

both chains A and C. For comparison purposes, similar perturbations and calculations were performed on respective different regions of the VH3 variant and used as the reference.

RESULTS

Effect of VH FWRs on FcεRIα binding

We produced all 7 VH1–VH7 family variants of pertuzumab IgE and collected only the corresponding monomeric fractions (green line in Fig E2 in this article's Online Repository at www.jacionline.org) for further analysis. Although some small shoulder peaks were observed (see Fig E2), we did not observe any significant aggregation patterns associated with any specific VH family variants. Minor batch variations were observed, although this was expected of transient transfection batches, which is a widely used method for producing biologics up to the preclinical stage.[47] For the trastuzumab IgE variants, only VH3, VH5, and VH7 family variants were produced in sufficient quantities for cross-checking experiments on FcεRIα.

All 7 pertuzumab IgE variants interacted strongly with the biosensor preloaded with Her2 (Fig 2), with the VH2 variant exhibiting the highest KD (weakest interaction). This finding was consistent with the pattern observed in our previously published data[32] on IgG_1 with the same V-regions, noting that in our previous IgG_1 experiment, pertuzumab VH2 IgG_1 had very poor responses.[32] Pertuzumab VH5 IgE variant had a lower dissociation rate constant and thus the lowest KD (0.23×10^{-10} mol/L, strongest interaction) to its antigen Her2 within the pertuzumab VH IgE panel (Fig 2).

In measurements of pertuzumab IgE variants to FcεRIα (which binds to the IgE Fc region),[48,49] all 7 pertuzumab VH variants interacted expectedly with FcεRIα. The pertuzumab VH5 IgE variant again exhibited the lowest KD (best interaction) at 0.66×10^{-10} mol/L because of its lower dissociation rate constant (Fig 3, *A*, and see Table E1 in this article's Online Repository at www.jacionline.org). Compared with the rest of the pertuzumab VH IgE variants, the VH6 variant had the highest KD (weakest interaction) to FcεRIα at 10.6×10^{-10} mol/L.

Because we previously demonstrated allosteric communications between the V- and C-regions on IgAs[30] and such an effect was also reported on IgGs by many other research groups,[26-29] we next sought to study whether such allosteric effects explained the differences in FcεRIα binding present in our pertuzumab IgE variants. To do this, we computationally modeled the full-length structures of all the pertuzumab IgE variants and quantified the allosteric communications between the V- and C-regions by using the AlloSigMA server (Fig 3, *B*).[45] Our results showed that there were allosteric communications between the V- and C-regions in all the pertuzumab IgE variants and that perturbation signaling at the V-regions could be propagated to the FcεRIα-binding site. As shown in the pertuzumab VH3 IgE variant, the allosteric communication contributed to increasing the dynamics at the FcεRIα-binding site (with $\Delta g_{FcεRIα} > 0$ in Fig 3, *B*) and hence the flexibility of the site. In particular, the most notable patterns of increase were observed in the pertuzumab VH4 and VH5 IgE variants. This was consistent with experimental measurements in which our pertuzumab VH5 IgE had the lowest KD to FcεRIα (shown in Fig 3, *A*, and see Table E1).

To investigate whether the CDRs influenced FcεRIα binding or whether the effect was solely due to specific VH FWRs, we grafted trastuzumab CDRs (which was fairly similar to pertuzumab to narrow down as many confounding variables as possible)[32] into the same VH FWRs to generate trastuzumab VH family IgE variants paired with the original trastuzumab light chain. Of the few trastuzumab VH IgE variants (VH3, VH5, and VH7) that could be produced in useable quantities, we observed a different KD pattern from the pertuzumab VH IgE variants. In contrast to the pertuzumab VH5 IgE variant exhibiting the lowest KD (Fig 3), the trastuzumab VH3 IgE was the VH variant with the lowest KD in the trastuzumab panel, although this was followed by trastuzumab VH5 IgE (Fig 4). This cross-check with pertuzumab IgE showed that the V-region effect on the C-region is elicited not by VH FWRs alone but involved the CDRs and possibly the light chain V-regions.

Because the binding interfaces between IgE-Fc to FcεRIα and to omalizumab shared a few neighboring residues (eg, P426 and R427 of chain C),[9] we next investigated whether the effect extended to omalizumab binding. Using our in-house recombinant omalizumab (synthesized based on a previous report[5]), we found no significant differences in KD values of the omalizumab interaction to all 7 variants of pertuzumab IgE (Fig 5, *A*). Furthermore, computational quantification of allosteric communications between the VH FWR and the omalizumab-binding site (Fig 5, *B*) showed differing responses from those of the FcεRIα-binding site. Unlike FcεRIα binding (which occurs asymmetrically[50]), omalizumab binding involves 2 Fab domains that bind symmetrically to the IgE Fc region (illustrated in Figs 3, *B*, and 5, *B*). This implies that

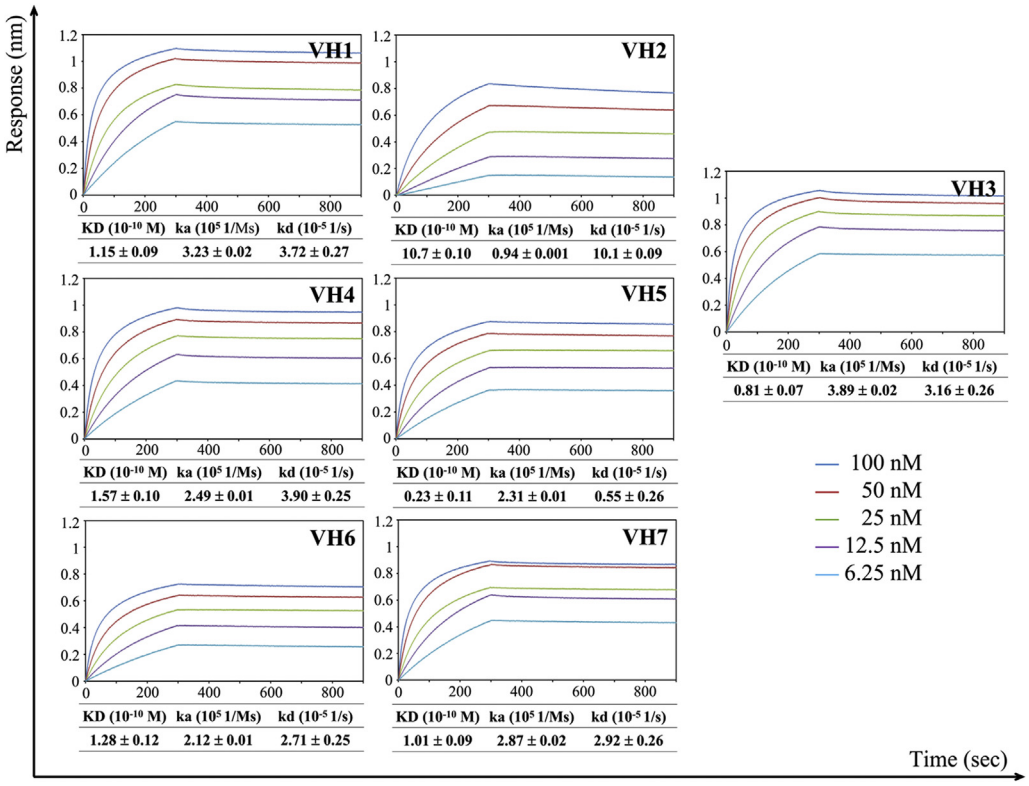

FIG 2. Biolayer interferometry measurements of pertuzumab VH IgE variants interacting with Her2. Antibodies at different concentrations were bound to the Her2 preloaded on Ni-NTA biosensors. KD, ka, and kd values were measured and calculated by using the Octet RED96 system. The *x-axis* depicts the time in seconds, and the *y-axis* depicts the response in nm.

the propagated signaling might have been more balanced and distributed between the 2 omalizumab-binding sites, resulting in insignificant varying responses to the omalizumab binding among the variants, as observed by using experimental measurements (Fig 5, *B*).

Effect of VH FWRs on spA binding

The superantigen spA was previously reported to bind specifically only to VH3 family antibodies[21-24]; however, none of our pertuzumab VH IgE variants (including the original VH3 pertuzumab sequence) interacted with spA (see Fig E3 in this article's Online Repository at www.jacionline.org). On the other hand, spA interacted strongly with our recombinant trastuzumab VH3 IgE variant, which had a similar FWR of the same VH3 family while also sharing the same Cε.

To further investigate the spA and VH interaction[21,39,40] that is independent of the light chain[40] or the constant heavy chain 1 domain,[51] we used the 2 available IgG_1^{Fab} crystal structures of trastuzumab (PDB: 1N8Z chain B) and pertuzumab (PDB: 1S78 chain D) to simulate interactions with spA. The structure of the IgM^{Fab}/spA complex (PDB: 1DEE) was used as a template. The best 4 structures of each resulting docked complex determined by using the HADDOCK2.2 server (which obtained similar binding modes to those in the referenced 1DEE structure)[38] were retrieved and found to agree with our experimental findings (Fig 6, *A*). As shown in Fig 6, *B*, spA interactions with pertuzumab VH3 region had scores that overlapped with those of the nonbinder (which is a biased docked complex of spA and IgM^{VL}).

The 3 VH regions (trastuzumab, pertuzumab, and the reference structure 1DEE) shared 12 of 13 identical residues at the spA-binding interface, except for the residue S58 in pertuzumab, which was uncommon among the known VH3 family germline sequences.[21] A point mutation at this position was previously reported[40] to disrupt spA binding because of opposite-charge repulsion from K58E. Nonetheless, this position was considered noncrucial and even mutation affordable[21] for spA binding with the other coexisting interacting residues in VH FWR1 and VH FWR3.[40] In our experiments, this residue (S58, located in the VH CDR2) was the only differing residue in the spA-binding region among the 3 antibody models (Fig 6, *C*), and although trastuzumab (with T58) could elicit spA binding (a conclusion made on structural alignment to the reference structure 1DEE with K58), the S58 residue alone in pertuzumab likely abrogated spA binding (Fig 6, *A* and *B*).

Electrostatic potential map of the interacting interfaces (Fig 6, *D*)[52,53] of the IgM^{Fab}/spA complex (PDB: 1DEE) regions showed the predominant electrostatic interaction, with positive charges on the VH surface. This positive potential (>0 kT/e) was also observed for the trastuzumab interface. However, when analyzing the pertuzumab VH3 surface, negative potential was spotted around the S58 residue (observed in all the 4 best docked complexes), which possibly repelled the spA binding.

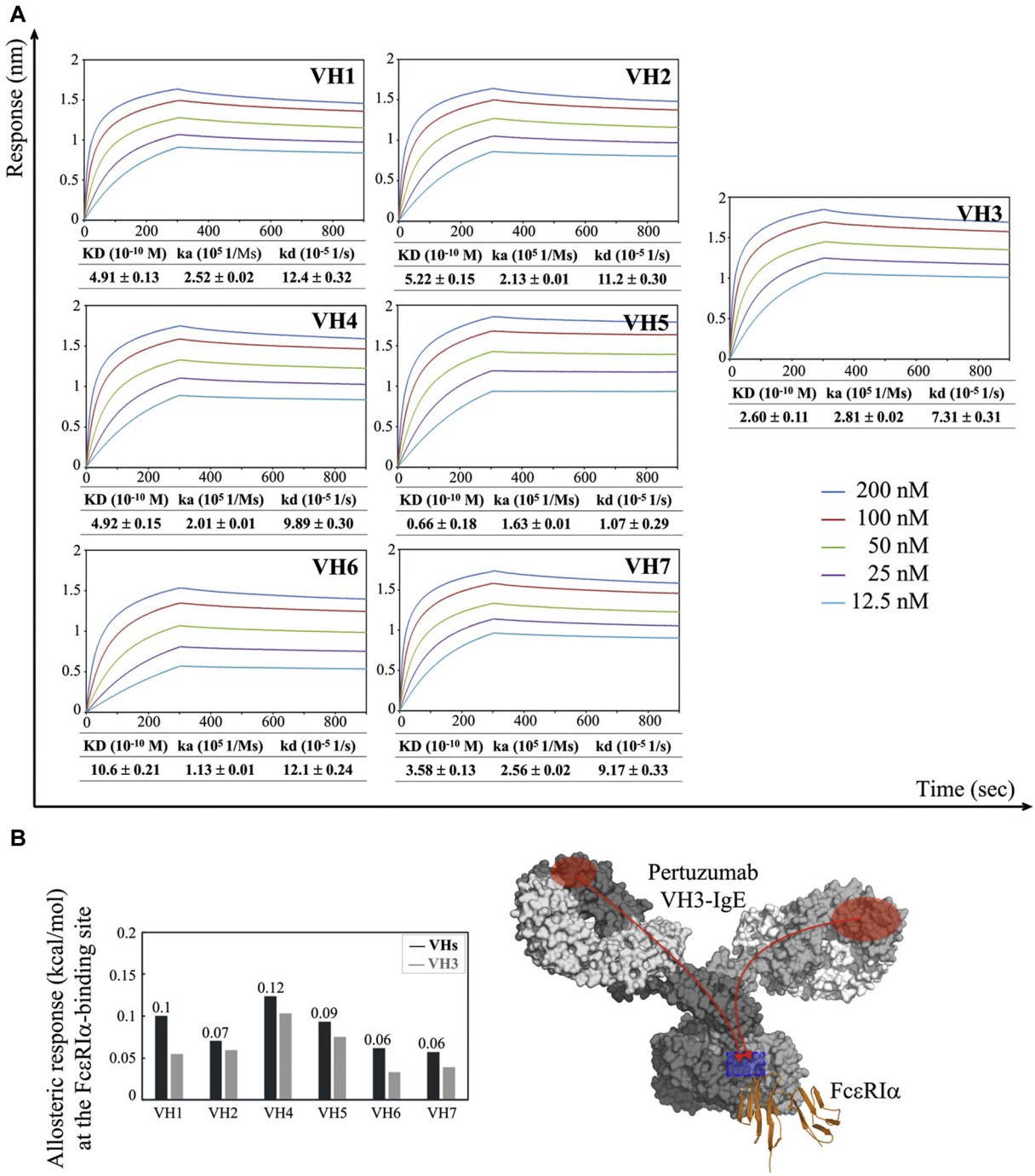

FIG 3. Interactions of pertuzumab VH IgE variants with FcεRIα. **A,** Biolayer interferometry measurements of pertuzumab VH IgE variants (VH1–VH7 at different concentrations) to FcεRIα preloaded on Ni-NTA biosensors. KD, ka, and kd values were measured and calculated by using the Octet RED96 system. **B,** Quantified allosteric communications between different VH FWRs and the FcεRIα-binding site. Structural surface presentation of the pertuzumab IgE VH3 variant is shown with highlighted VH FWRs (red) and the FcεRIα-binding site (blue). For illustration purposes, the FcεRIα domain (presented in orange) was placed near the FcεRIα-binding site by superimposing the full-length IgE model with the bound IgE^{Fc}/FcεRIα complex structure (PDB: 2Y7Q).

In measurement of residue-wise contribution to total binding energy (Fig 6, *C*), residue S58 was less likely to contribute to the binding, whereas the other 2 antibody VH surfaces had more contributing residues.

DISCUSSION

We sought to explore the effect of IgE VH FWRs on FcεRIα, Her2, anti-IgE omalizumab, and spA binding by using anti-Her2 pertuzumab CDRs. Pertuzumab was used as a model because it is

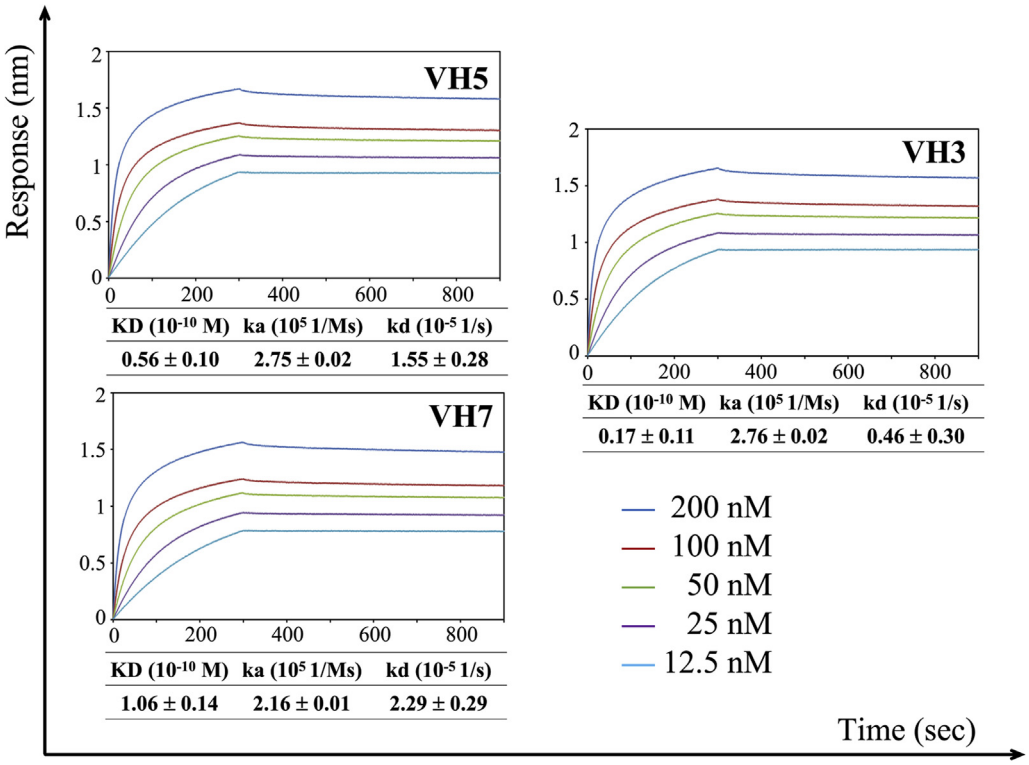

FIG 4. Biolayer interferometry measurements of trastuzumab VH IgE variants with FcεRIα. Trastuzumab VH IgE variants (VH3, VH5, and VH7 at different concentrations) to FcεRIα preloaded on Ni-NTA biosensors were measured. KD, ka, and kd values were calculated by using the Octet RED96 system. The other trastuzumab VH IgE variants (VH1, VH2, VH4, and VH6) were not produced in measurable quantities.

a well-studied therapeutic antibody and for its potential in allergo-oncology.

To study the effects of VH family FWRs, representative FWR germline sequences of VH1–VH7 with the exception of VH3 (using the original pertuzumab VH3 sequence) were used. Within the VH variants, all variants exhibited expected association and dissociation rates to Her2, with the exception of the pertuzumab VH2 IgE variant, which had weaker binding properties to Her2. Nonetheless, this was expected because it was of a similar trend to our previous data on IgG_1[32] using the same V-regions.

In production of the recombinant representative VH family pertuzumab IgE variants, we also investigated whether VH FWRs would lead to different aggregation patterns and thereby exhibit possible monomeric activation of allergic effect cells (ie, the "cytokinergic effect"), as reported for the rodent IgE SPE7.[4] Based on our size exclusion chromatography results of the purified pertuzumab IgE variants, we did not find notable aggregation trends for any of the VH family representatives in our purification conditions, nor was there evidence for natural polymerization as in the case for IgM.[31,54]

Our previous work on IgG_1[32] showed the VH family FWRs to have effects on FcγRIIA. To determine whether VH family FWRs have the same effect on IgE to FcεRIα, which has clear implications on type I hypersensitivity and engineering of IgE therapeutics, we found such an effect in 1 of 10 of our recombinant IgEs. Our pertuzumab VH5 IgE variant exhibited the lowest KD value to FcεRIα with the slowest dissociation among the pertuzumab variants, but this was not solely due to the VH FWRs because such effects were absent for our trastuzumab VH5 IgE. Both the trastuzumab VH3 and VH5 variants exhibited similar KD values, with little difference between the VH FWRs within the panel. Thus differences between the 2 VH3 IgE variants suggest FcεRIα engagement on the C-region to be an effect arising from both CDRs and FWRs or the whole VH, if not the whole V-region involving both the heavy and light chains. From this, we propose that the presence of such persistent IgEs with V-regions that extended FcεRIα engagement in patient repertoires might be an underlying IgE-mediated allergy pathogenesis, depending on the antigen and specificity of such IgEs.

We speculate the prolonged interaction to FcεRIα to lead to the emergence and overpresentation of these persistent IgEs against a heterogeneous microenvironment of higher dissociative IgEs by simply being more persistent. Given that such effects are likely due to a combination of factors within the V-regions of IgE rather than specific VH FWRs, it would be difficult to predict what type of persistent IgE might become the dominant type in the local environment. Thus future allergen-specific IgE studies and engineering of therapeutic IgEs would benefit from analyzing specific IgEs as a whole rather than as a sum of regions or domains.[55] Although we were able to artificially create a more persistent IgE with V-regions that augmented FcεRIα engagement in the rare pertuzumab VH5 IgE (the only of 10 recombinant IgEs we produced), the discovery for such a patient-derived IgE would certainly change the understanding of the role of IgE V-regions in allergy pathogenesis.

The effect of the pertuzumab VH5 variant on FcεRIα engagement, which is independent of engagement with omalizumab, also has implications for anti-IgE treatment. Because high

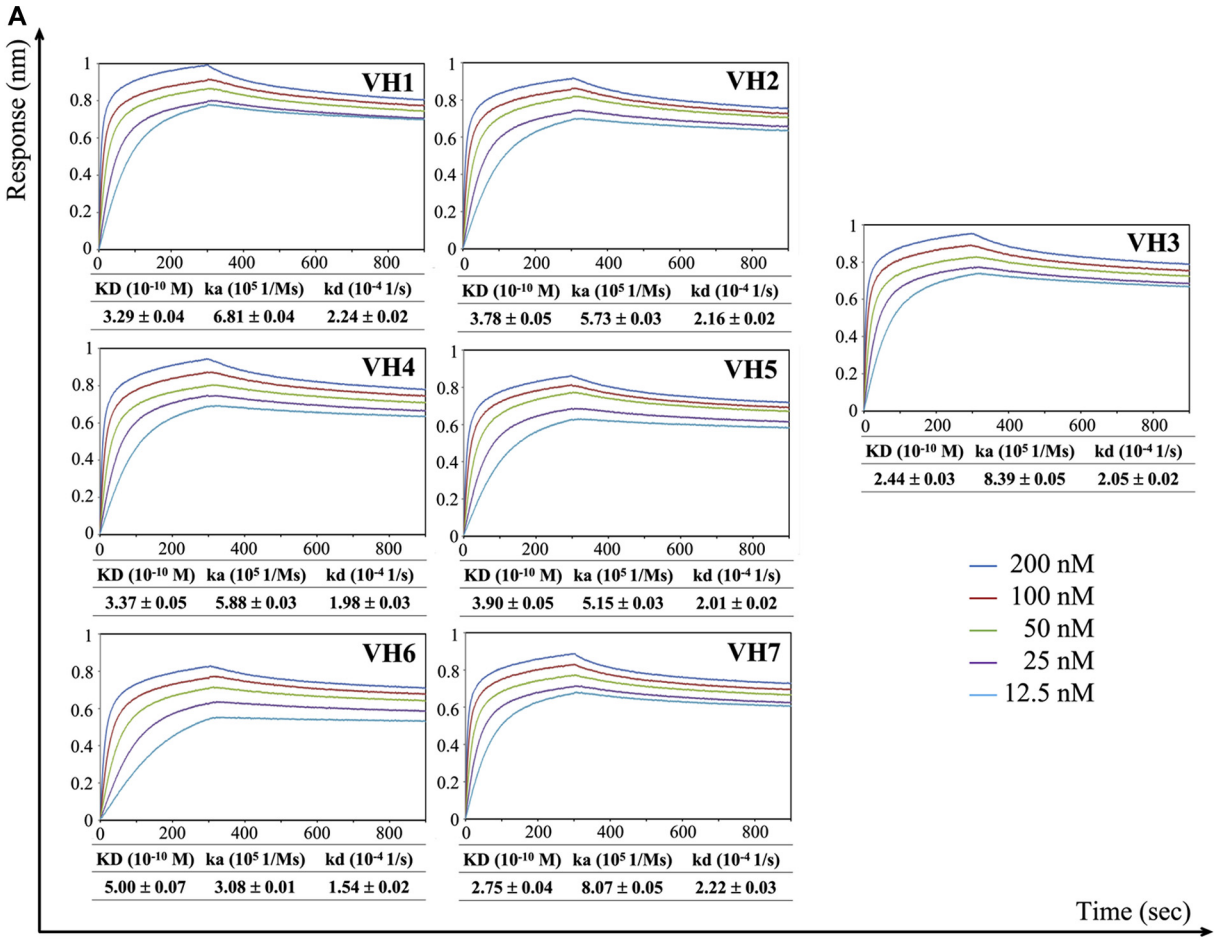

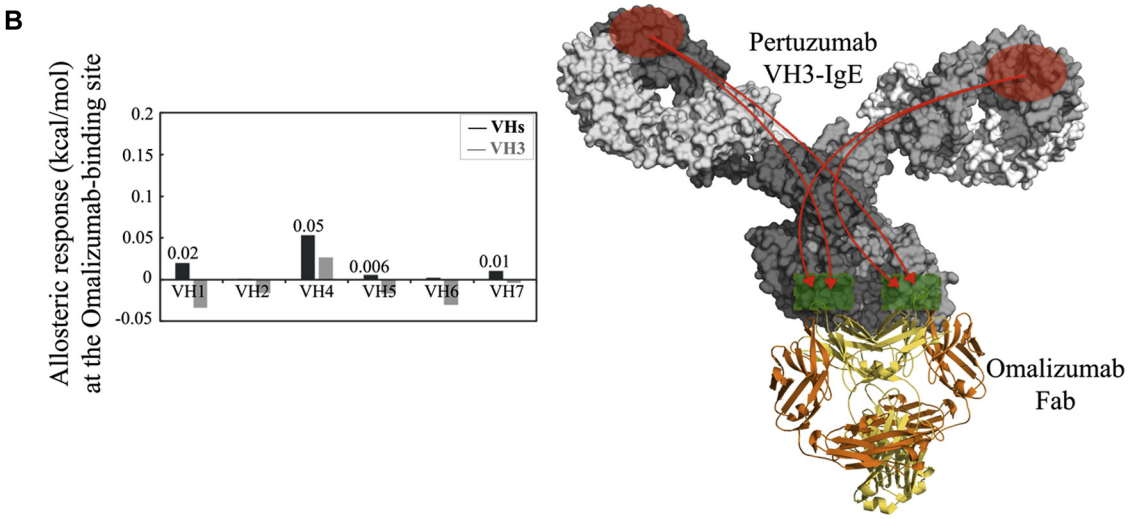

FIG 5. Interactions of pertuzumab VH IgE variants with anti-IgE antibody (omalizumab). **A,** Biolayer interferometry measurements of pertuzumab VH IgE variants (VH1–VH7 at different concentrations) to omalizumab preloaded on Anti-hIgG-Fc Capture biosensors. KD, ka, and kd values were measured and calculated by using the Octet RED96 system. **B,** Quantified allosteric communications between different VH FWR regions and the omalizumab-binding site. Structural surface presentation of the pertuzumab IgE VH3 variant is shown with highlighted VH FWRs (red) and the omalizumab-binding site (green). For illustration purposes, the omalizumab Fab domains (presented in orange and yellow) were placed near the omalizumab-binding site by superimposing the full-length IgE model with the bound IgE^{Fc}/omalizumab complex structure (PDB: 5HYS).

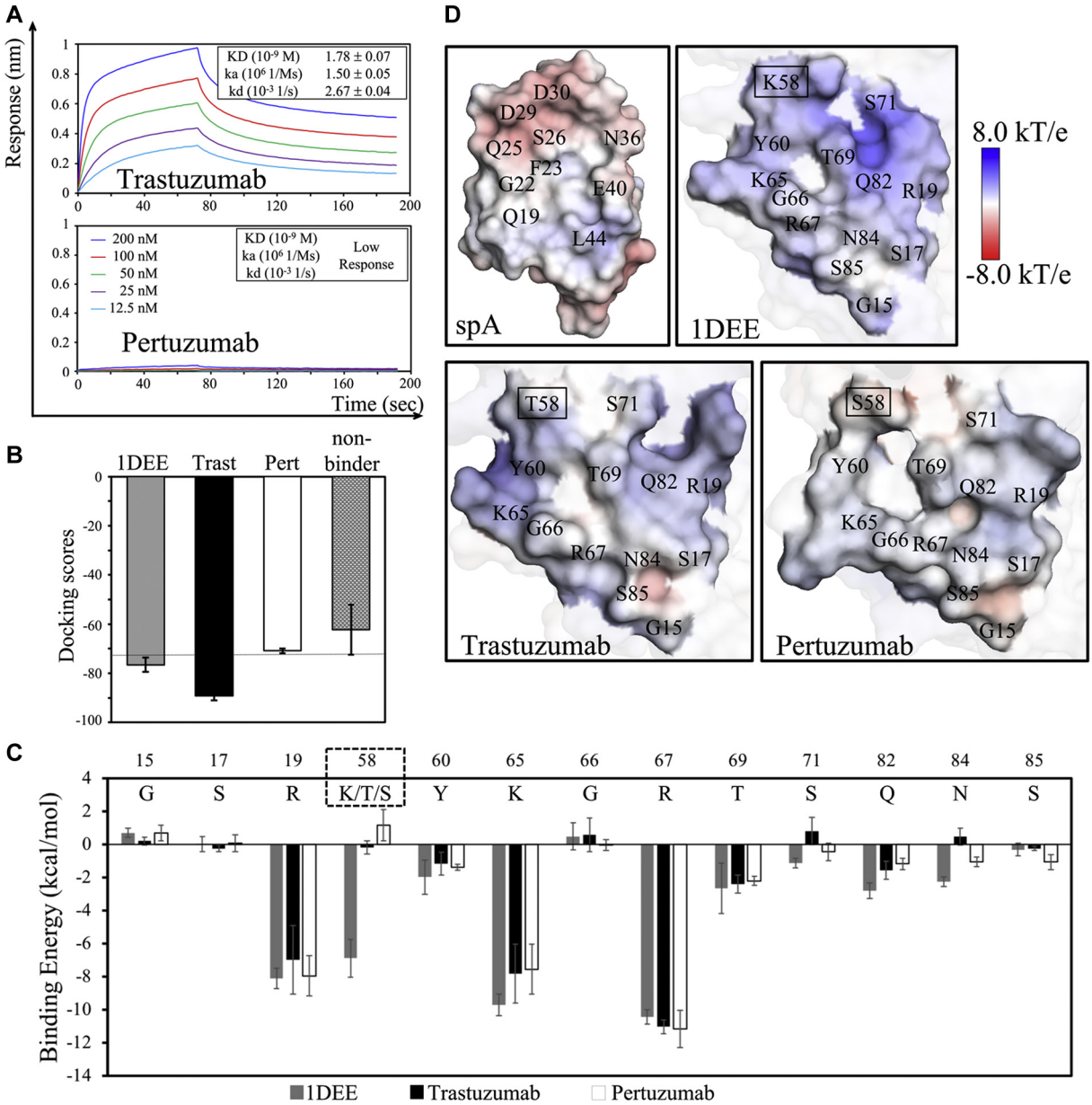

FIG 6. Analyses of spA binding to trastuzumab and pertuzumab VH regions. **A,** Results of spA binding to the 2 IgE antibodies. **B,** Computational docking scores showed the pertuzumab VH to have similar results with those of the nonbinder. **C,** Contribution of interfacial residues on total binding energy of the 3 antibody VH regions with spA. **D,** Electrostatic potential map of the interfaces of spA and those of the 3 antibody VH regions. Electrostatic surfaces were generated by using PyMOL[52] and the APBS plugin. An augmented reality presentation of the IgM^{Fab}/spA complex (PDB: 1DEE) could be viewed using our "APD AR Holistic Review" app available on both Google and Apple app stores (for more details see Poh et al[53]).

concentrations of omalizumab were reported to dissociate the preformed IgE-FcεRIα complex *in vitro* and slowly *ex vivo*,[8] low dissociating FcεRIα-bound persistent IgE might yet be more resistant than IgEs of other VH families.

Within a closed energy system, the modulating allosteric communication (Fig 3, *B*) between the FcεRIα-binding site and pertuzumab VH5 FWRs would be a compensation to the increased flexibility conferred by VH5 FWRs at V-regions. Interestingly, V-region flexibility was constrained by the other arm of the V-region because of asymmetric bending in IgE[50] induced by FcεRIα binding. This resulted in an overall less flexible IgE structure, a finding previously discussed by Holdom et al.[50] We found this compensation phenomenon to be present in all our pertuzumab VH variants (see Fig E4 in this article's Online Repository at www.jacionline.org). In addition, disrupting sites in VH FWRs (eg, mutating to alanine) rendered the FcεRIα-binding site more flexible, showing that VH FWRs contribute to stabilizing the FcεRIα-binding site and hence facilitate and maintain the interaction. This trend of effects in which VH regions modulated FcεRIα binding (Fig 3, *A*) was observed in all our pertuzumab VH variants in varying extents (Fig 3, *B*).

Given reports that the presence of *Staphylococcus aureus* is associated with allergic rhinitis,[56,57] there were hypotheses that superantigen, such as spA, by *S aureus* or other colonizing microorganisms might activate polyclonal IgE.[58-60] Given our observations of pertuzumab VH5 IgE, it would certainly be exciting whether IgEs with such V-regions could interact nonspecifically with superantigens. Apart from being a known superantigen to activate mast cells,[22] spA has also been exploited for antibody purification industrially.[20] Nonetheless, we did not find any of our pertuzumab VH IgE variants to bind spA (see Fig E3), including our pertuzumab VH3 variant. This was in contrast to our recombinant trastuzumab IgE of original VH3 FWRs, which interacted with spA (Fig 6, *A*). Taking into account our results that were congruent with previous reports that spA did not bind IgE Fc,[61,62] our analysis of the sequence and structural models showed the pertuzumab VH3 IgE to be slightly different from the known binding VH3 through its distinct residue S58 located at VH CDR2, which repelled spA at the interface.[39] Because the mutation was within VH CDR2, which is likely to have a smaller effect on antigen binding than VH CDR3,[63] there is minimal disruption to using optimized VH3 FWRs in biotechnological manufacturing. Thus there is the option to engineer spA binding properties in recombinant antibodies, whether it be for purification (using trastuzumab VH3 FWR in grafting) or to abolish spA binding for therapeutic purposes (using the pertuzumab CDR2 mutation). This finding is of value to the biotech industry given that VH3 FWRs were found to yield higher antibody production rates.[32,64,65]

Our findings of trastuzumab IgE binding to spA (Fig 6, *A*) brings caution to the use of trastuzumab IgE in allergoncology[66] because of its potential nonspecific activation elicited by spA, particularly in mucosal regions that might have exposure to spA from *S aureus*,[14,60] leading to possible anaphylaxis. Thus, with spA therapy (in clinical trials for immune thrombocytopenia and rheumatoid arthritis),[67] care must be taken that any accompanying therapeutic antibody should be engineered to prevent interactions.

On this aspect, pertuzumab (also of VH3 origin) might be a better candidate for Her2-targetted allergo-oncology than trastuzumab, especially when targeting mucosal areas (whereas blood and many internal organs are typically free of microorganisms and their proteins). Regardless, the promise of therapeutic IgE antibodies[68] is still great and exciting, and although the findings here raised some cause for concern, a potential solution of modifying S58 is also proposed.

In conclusion, we have shown a possible effect of increasing FcεRIα interaction by IgE caused by the VH regions through a possible underlying allosteric communication between the V- and C-regions. In addition, we have also characterized VH family–associated effects on antigen/superantigen binding that is relevant to the design of IgE therapeutics.

The molecular dynamics simulations of all the pertuzumab IgE VH variants were performed on the petascale computer cluster ASPIRE-1 at the National Supercomputing Center of Singapore.

Clinical implications: IgE-VH family effects were found for FcεRIα but not omalizumab interactions, with a possible role in allergy. On allergo-oncology therapeutics, designing non–spA-binding IgEs might be necessary for clinical safety.

REFERENCES

1. Gould HJ, Sutton BJ. IgE in allergy and asthma today. Nat Rev Immunol 2008;8:205-17.
2. Akin C. Mast cell activation syndromes. J Allergy Clin Immunol 2017;140:349-55.
3. Kawakami T, Kitaura J. Mast cell survival and activation by IgE in the absence of antigen: A consideration of the biologic mechanisms and relevance. J Immunol 2005;175:4167-73.
4. Bax H, Bowen H, Dodev TS, Sutton BJ, Gould HJ. Mechanism of the antigen-independent cytokinergic SPE-7 IgE activation of human mast cells in vitro. Sci Rep 2015;5:9538.
5. Wright JD, Chu HM, Huang CH, Ma C, Chang TW, Lim C. Structural and physical basis for anti-IgE therapy. Sci Rep 2015;5:11581.
6. Beck LA, Marcotte GV, MacGlashan D, Togias A, Saini S. Omalizumab-induced reductions in mast cell FcεRI expression and function. J Allergy Clin Immunol 2004;114:527-30.
7. Prussin C, Griffith DT, Boesel KM, Lin H, Foster B, Casale TB. Omalizumab treatment downregulates dendritic cell FcεRI expression. J Allergy Clin Immunol 2003;112:1147-54.
8. Eggel A, Baravalle G, Hobi G, Kim B, Buschor P, Forrer P, et al. Accelerated dissociation of IgE:FcεRI complexes by disruptive inhibitors actively desensitizes allergic effector cells. J Allergy Clin Immunol 2014;133:1709-19.e8.
9. Pennington LF, Tarchevskaya S, Brigger D, Sathiyamoorthy K, Graham MT, Nadeau KC, et al. Structural basis of omalizumab therapy and omalizumab-mediated IgE exchange. Nat Commun 2016;7:11610.
10. Janezic A, Chapman CJ, Snow RE, Hourihane JO, Warner JO, Stevenson FK. Immunogenetic analysis of the heavy chain variable regions of IgE from patients allergic to peanuts. J Allergy Clin Immunol 1998;101:391-6.
11. Snow RE, Djukanovic R, Stevenson FK. Analysis of immunoglobulin E VH transcripts in a bronchial biopsy of an asthmatic patient confirm bias towards VH5, and indicates local clonal expansion, somatic mutation and isotype switch events. Immunology 1999;98:646-51.
12. Snow RE, Chapman CJ, Frew AJ, Holgate ST, Stevenson FK. Analysis of Ig VH region genes encoding IgE antibodies in splenic B lymphocytes of a patient with asthma. J Immunol 1995;154:5576-81.
13. Coker HA, Harries HE, Banfield GK, Carr VA, Durham SR, Chevretton E, et al. Biased use of VH5 IgE-positive B cells in the nasal mucosa in allergic rhinitis. J Allergy Clin Immunol 2005;116:445-52.
14. Chen JB, James LK, Davies AM, Wu YB, Rimmer J, Lund VJ, et al. Antibodies and superantibodies in patients with chronic rhinosinusitis with nasal polyps. J Allergy Clin Immunol 2017;139:1195-204.e11.
15. Lim A, Luderschmidt S, Weidinger A, Schnopp C, Ring J, Hein R, et al. The IgE repertoire in PBMCs of atopic patients is characterized by individual rearrangements without variable region of the heavy immunoglobulin chain bias. J Allergy Clin Immunol 2007;120:696-706.
16. Davies JM, O'Hehir RE. VH gene usage in immunoglobulin E responses of seasonal rhinitis patients allergic to grass pollen is oligoclonal and antigen driven. Clin Exp Allergy 2004;34:429-36.
17. Bando Y, Shimizu A, Ra C. Characterization of VHε gene expressed in PBL from children with atopic diseases: detection of homologous VH1-69 derived transcripts from three unrelated patients. Immunol Lett 2004;94:99-106.
18. Eibensteiner P, Spitzauer S, Steinberger P, Kraft D, Valenta R. Immunoglobulin E antibodies of atopic individuals exhibit a broad usage of VH-gene families. Immunology 2000;101:112-9.
19. Tilgner J, Golembowski S, Kersten B, Sterry W, Jahn S. VH genes expressed in peripheral blood IgE-producing B cells from patients with atopic dermatitis. Clin Exp Immunol 1997;107:528-35.
20. Darcy E, Leonard P, Fitzgerald J, Danaher M, Ma H, O'Kennedy R. Purification of antibodies using affinity chromatography. In: Walls D, Loughran S, editorsProtein chromatography. Methods in molecular biology. New York: Humana Press; 2017. pp. 305-18.
21. Graille M, Stura EA, Corper AL, Sutton BJ, Taussig MJ, Charbonnier J-B, et al. Crystal structure of a *Staphylococcus aureus* protein A domain complexed with the Fab fragment of a human IgM antibody: structural basis for recognition of B-cell receptors and superantigen activity. Proc Natl Acad Sci U S A 2000;97:5399-404.
22. Genovese A, Bouvet J-P, Florio G, Lamparter-Schummert B, Bjorck L, Marone G. Bacterial immunoglobulin superantigen proteins A and L activate human heart mast cells by interacting with immunoglobulin E. Infect Immun 2000;68:5517-24.
23. Silverman GJ, Pires R, Bouvet JP. An endogenous sialoprotein and a bacterial B cell superantigen compete in their VH family-specific binding interactions with human Igs. J Immunol 1996;157:4496-502.
24. Hillson JL, Karr NS, Oppliger IR, Mannik M, Sasso EH. The structural basis of germline-encoded VH3 immunoglobulin binding to staphylococcal protein A. J Exp Med 1993;178:331-6.

25. Zhao J, Nussinov R, Ma B. Allosteric control of antibody-prion recognition through oxidation of a disulfide bond between the CH and CL chains. Protein Eng Des Sel 2017;30:67-76.
26. Zhao J, Nussinov R, Ma B. Antigen binding allosterically promotes Fc receptor recognition. MAbs 2019;11:58-74.
27. Yang D, Kroe-Barrett R, Singh S, Roberts CJ, Laue TM. IgG cooperativity—is there allostery? Implications for antibody functions and therapeutic antibody development. MAbs 2017;9:1231-52.
28. Janda A, Bowen A, Greenspan NS, Casadevall A. Ig constant region effects on variable region structure and function. Front Microbiol 2016;7:22.
29. Oda M, Kozono H, Morii H, Azuma T. Evidence of allosteric conformational changes in the antibody constant region upon antigen binding. Int Immunol 2003;15:417-26.
30. Su CTT, Lua WH, Ling WL, Gan SKE. Allosteric effects between the antibody constant and variable regions: a study of IgA Fc mutations on antigen binding. Antibodies 2018;7:20.
31. Lua WH, Ling WL, Yeo JY, Poh JJ, Lane DP, Gan SKE. The effects of antibody engineering CH and CL in trastuzumab and pertuzumab recombinant models: impact on antibody production and antigen-binding. Sci Rep 2018;8:718.
32. Ling WL, Lua WH, Poh JJ, Yeo JY, Lane DP, Gan SKE. Effect of VH-VL families in pertuzumab and trastuzumab recombinant production, Her2 and FcγIIA binding. Front Immunol 2018;9:469.
33. Gan SKE, Hunt J, Marsh PJ, Beavil AJ, Harries HE. The rapid expression of human immunoglobulins. Patent UK0810633.8 and US61/060.239. 2008.
34. Chan WT, Verma CS, Lane DP, Gan SKE. A comparison and optimization of methods and factors affecting the transformation of *Escherichia coli*. Biosci Rep 2013;33:e00086.
35. Poh JJ, Gan SKE. The determination of factors involved in column-based nucleic acid extraction and purification. J Bioprocessing Biotechniques 2014;4:157.
36. Su CTT, Ling WL, Lua WH, Poh JJ, Gan SKE. The role of antibody Vκ framework 3 region towards antigen binding: effects on recombinant production and protein L binding. Sci Rep 2017;7:3766.
37. Lua WH, Gan SKE, Lane DP, Verma CS. A search for synergy in the binding kinetics of trastuzumab and pertuzumab whole and F (ab) to Her2. NPJ Breast Cancer 2015;1:15012.
38. van Zundert GCP, Rodrigues JPGLM, Trellet M, Schmidt C, Kastritis PL, Karaca E, et al. The HADDOCK2.2 webserver: user-friendly integrative modeling of biomolecular complexes. J Mol Biol 2015;428:720-5.
39. Randen I, Potter KN, Li Y, Thompson KM, Pascual V, Forre O, et al. Complementarity-determining region 2 is implicated in the binding of staphylococcal protein A to human immunoglobulin VHIII variable regions. Eur J Immunol 1993;23:2682-6.
40. Potter KN, Li Y, Pascual V, Capra JD. Staphylococcal protein A binding to VH3 encoded Immunoglobulins. Intern Rev Immunol 1997;14:291-308.
41. Hess B, Kutzner C, Van der Spoel D, Lindahl E. GROMACS 4: algorithms for highly efficient, load-balanced, and scalable molecular simulation. J Chem Theory Comp 2008;4:435-47.
42. Kumari R, Kumar R, Open Source Discovery Consortium, Lynn A. g_mmpbsa—a GROMACS tool for high-throughput MM-PBSA calculations. J Chem Inf Model 2014;54:1951-62.
43. Baker N, Sept D, Joseph S, Holst M, McCammon JA. Electrostatics of nanosystems: application to microtubules and the ribosome. Proc Natl Acad Sci U S A 2001;98:10037-41.
44. Krinov G, Shapovalov M, Dunbrack R. Improved prediction of protein side-chain conformations with SCWRL4. Proteins 2009;77:778-95.
45. Guarnera E, Tan Z-W, Zheng Z, Berezovsky IN. AlloSigMA: allosteric signaling and mutation analysis server. Bioinformatics 2017;33:3996-8.
46. Guarnera E, Berezovsky IN. Structure-based statistical mechanical model accounts for the causality and energetics of allosteric communications. PLoS Comput Biol 2016;12:e1004678.
47. Gutierrez-Granados S, Cervera L, Kamen AA, Godia F. Advancements in mammalian cell transient gene expression (TGE) technology for accerelated production of biologics. Crit Rev Biotechnol 2018;38:918-40.
48. Blank U, Ra CS, Kinet JP. Characterization of truncated α chain products from human, rat, and mouse high affinity receptor for immunoglobulin E. J Biol Chem 1991;266:2639-46.
49. Hakimi J, Seals C, Kondas JA, Pettine L, Danho W, Kochan J. The α subunit of the human IgE receptor (FcERI) is sufficient for high affinity IgE binding. J Biol Chem 1990;265:22079-81.
50. Holdom MD, Davies AM, Nettleship JE, Babgy SC, Dhaliwal B, Girardi E, et al. Conformational changes in IgE contribute to its uniquely slow dissociation rate from receptor FcεRI. Nat Struct Mol Biol 2011;18:571-6.
51. Sasso EH, Silverman GJ, Mannik M. Human IgA and IgG F(ab')2 that bind to staphylococcal protein A belong to the VHIII subgroup. J Immunol 1991;147:1877-83.
52. Schrodinger L. The PyMOL molecular graphics system. 2019. Available at: https://pymol.org/2/. Accessed March 25, 2019.
53. Poh JJ, Phua SX, Chan KF, Gan SKE. Commentary: augmented reality scientific phone apps—making the APD AR Holistic Review app and using existing AR apps for scientific publications. Scientific Phone Apps Mobile Devices 2018;4:4.
54. Wiersma EJ, Collins C, Fazel S, Shulman MJ. Structural and functional analysis of J chain-deficient IgM. J Immunol 1998;160:5979-89.
55. Phua SX, Chan KF, Su CTT, Poh JJ, Gan SKE. Perspective: the promises of a holistic view of proteins—impact on antibody engineering and drug discovery. Biosci Rep 2019;39:BSR20181958.
56. Shiomori T, Yoshida S, Miyamoto H, Makishima K. Relationship of nasal carriage of Staphylococcus aureus to pathogenesis of perennial allergic rhinitis. J Allergy Clin Immunol 2000;105:449-54.
57. Coscia GT, Perzanowski M, Smith H, Ryan C, Planet PJ. Nasal colonization with *S. aureus* is associated with allergic sensitization in children with chronic rhinitis [abstract]. J Allergy Clin Immunol 2018;141:AB280.
58. Rossi RE, Monasterolo G. Prevalence of serum IgE antibodies to the *Staphylococcus aureus* enterotoxins (SAE, SEB, SEC, SED, TSST-1) in patients with persistent allergic rhinitis. Int Arch Allergy Immunol 2004;133:261-6.
59. Bachert C, van Zele T, Gevaert P, De Schrijver L, Van Cauwenberge P. Superantigens and nasal polyps. Curr Allergy Asthma Rep 2003;3:523-31.
60. Zhang N, Holtappels G, Gevaert P, Patou J, Dhaliwal B, Gould H, et al. Mucosal tissue polyclonal IgE is functional in response to allergen and SEB. Allergy 2011;66:141-8.
61. Peng Z, Becker AB, Simons FER. Binding properties of Protein A and Protein G for human IgE. Int Arch Allergy Immunol 1994;104:204-6.
62. Inganas M, Johansson SG, Bennich HH. Interaction of human polyclonal IgE and IgG from different species with protein A from *Staphylococcus aureus*: demonstration of protein-A-reactive sites located in the Fab'2 fragment of human IgG. Scand. J Immunol 1980;12:23-31.
63. Xu JL, Davis MM. Diversity in the CDR3 region of V(H) is sufficient for most antibody specificities. Immunity 2000;13:37-45.
64. Ewert S, Hubert T, Honegger A, Pluckthun A. Biophysical properties of human antibody variable domains. J Mol Biol 2003;325:531-53.
65. Igawa T, Tsunoda H, Kuramochi T, Sampei Z, Ishii S, Hattori K. Engineering the variable region of therapeutic IgG antibodies. MAbs 2011;3:243-52.
66. Karagiannis P, Singer J, Hunt J, Gan SKE, Rudman SM, Mechtcheriakova D, et al. Characterization of an engineered trastuzumab IgE antibody and effector cell mechanisms targeting HER2/neu positive tumor cells. Cancer Immunol Immunother 2009;58:915-30.
67. Eftimiadi G, Vinai P, Eftimiadi C. Staphylococcal protein A as a pharmacological treatment for autoimmune disorders. J Autoimmune Disord 2017;3:40.
68. Penichet ML, Schultes BC, Nicodemus CF, Daniels TR, Helguera G, Rodriguez JA. IgE antibodies for the treatment of cancer. Patent 8697079, Quest Pharma Tech, Regents of the University of California; 2014.

```
                 -------------- FWR1 --------------- CDR1 ---------- FWR2 ------ CDR2 ------------------ FWR3 ------------------ CDR3 ------ FWR4 ----------------

 Pertuzumab_LC:  DIQMTQSPSSLSASVGDRVTITCKASQDVSIGVAWYQQKPGKAPKLLIYSASYRYTGVPSRFSGSGSGTDFTLTISSLQPEDFATYYCQQYYIYPYTFGQGTKVEIK
Trastuzumab_LC:  DIQMTQSPSSLSASVGDRVTITCRASQDVNTAVAWYQQKPGKAPKLLIYSASFLYSGVPSRFSGSRSGTDFTLTISSLQPEDFATYYCQQHYTTPPTFGQGTKVEIK
                                         *****   **                ***  *                                   ** *  *

 Pertuzumab_HC:EVQLVESGGGLVQPGGSLRLSCAASGFTFTDYTMDWVRQAPGKGLEWVADVNPNSGGSIYNQRFKGRFTLSVDRSKNTLYLQMNSLRAEDTAVYYCARNLGPSFY-FDYWGQGTLVTVSS
Trastuzumab_HC:EVQLVESGGGLVQPGGSLRLSCAASGFNIKDTYIHWVRQAPGKGLEWVARIYPTNGYTRYADSVKGRFTISADTSKNTAYLQMNSLRAEDTAVYYCSRWGGDGFYAMDYWGQGTLVTVSS
                                         **   *                  *   *  *   *    **                                  *  *  **  **
```

FIG E1. Sequence alignments of trastuzumab and pertuzumab variable heavy chains *(HC)* and light chains *(LC)*. CDRs are shown in boldface, with *asterisks* highlighting the identical residues between the 2 variant CDRs.

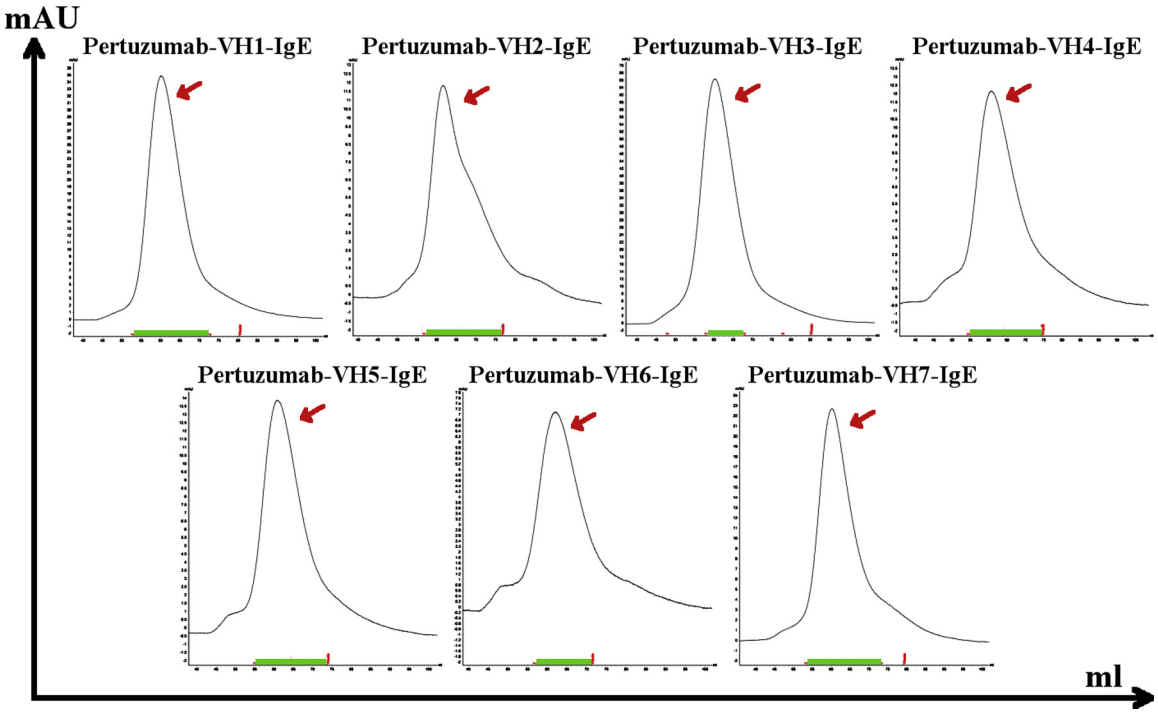

FIG E2. Size exclusion chromatography profiles of pertuzumab VH IgE variants using the Superdex S200 size exclusion column after affinity purification (Protein L column) with the AKTA Pure system. *x-axis*, Forty- to 100-mL time scale; *y-axis*, mAU absorption, as determined by using UV detection. *Green horizontal line on the x-axis* indicates the fractions collected.

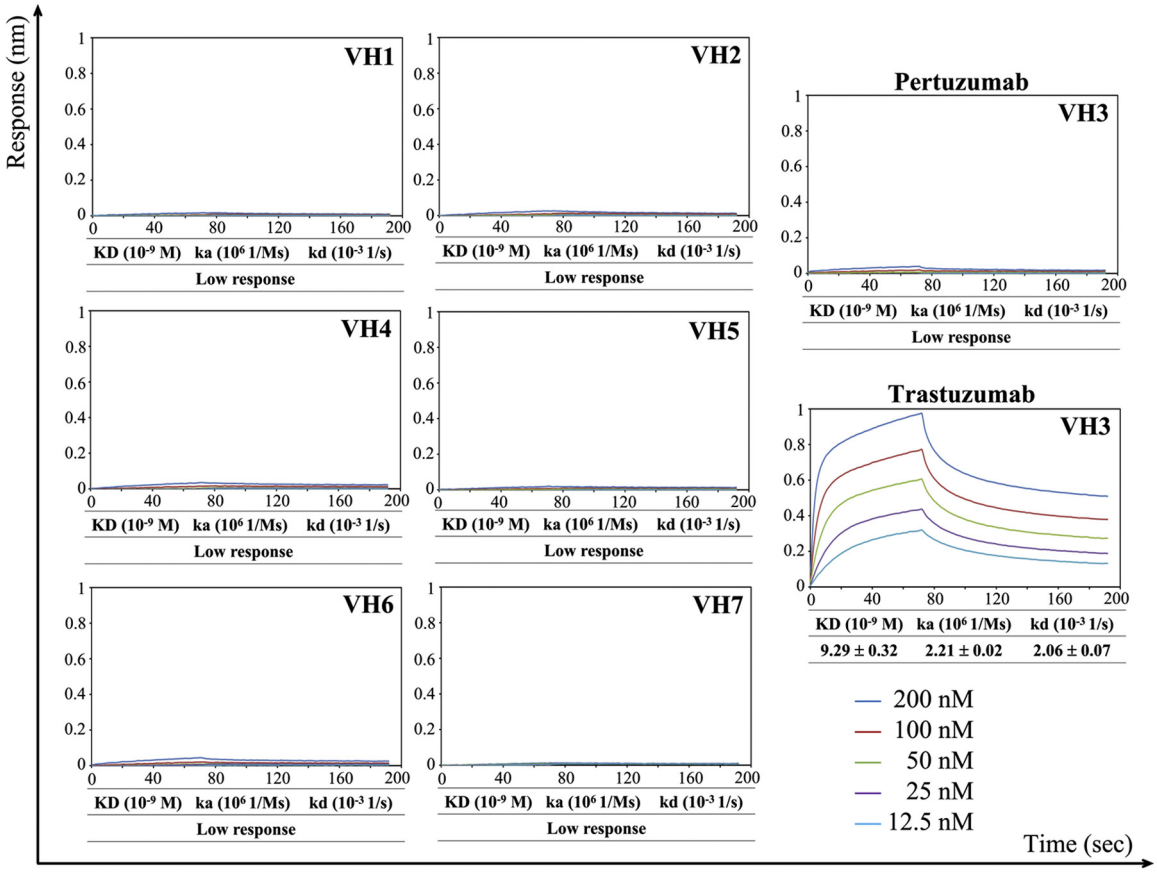

FIG E3. Biolayer interferometry measurements of pertuzumab VH IgE variants interacting with spA. Interactions (KD, ka, and kd) of pertuzumab VH IgE variants and trastuzumab VH3 IgE at concentrations from 100 to 12.5 nmol/L concentrations to protein A biosensors were measured and calculated by using the Octet RED96 system. The *x-axis* depicts time in seconds, and the *y-axis* depicts responses in nm.

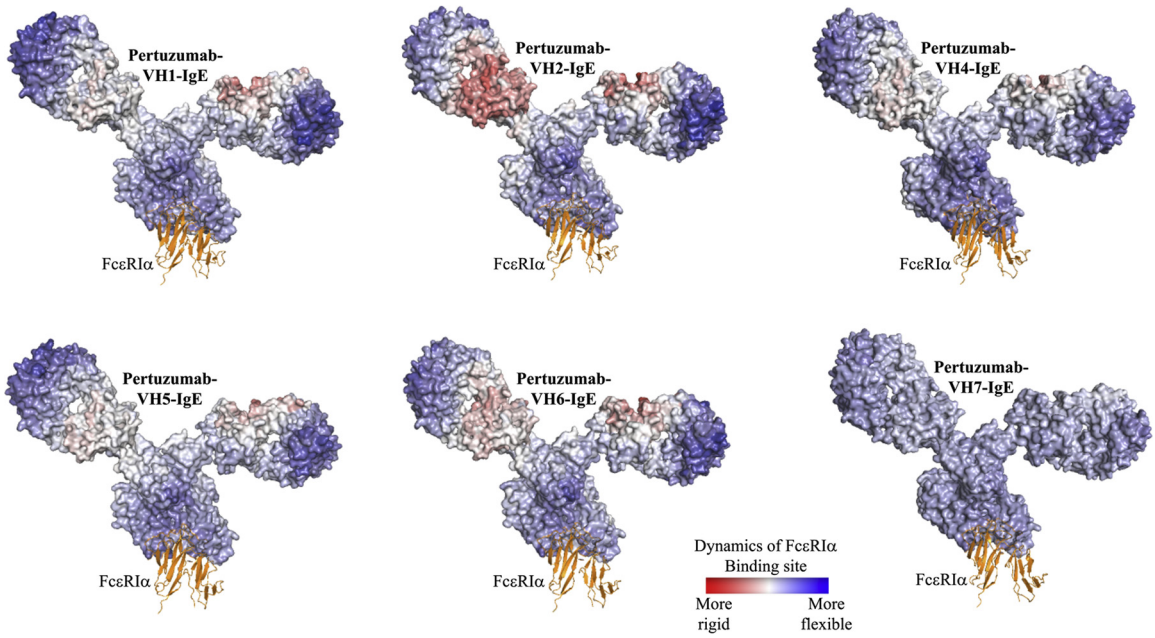

FIG E4. Allosteric communication between VH FWRs and the FcεRIα-binding site on pertuzumab IgE variants (except the wild-type VH3). Structural representatives of the variants are presented in surfaces and colored based on the allosteric responses (shown in Fig 3, *B*) compared with the pertuzumab IgE VH3. FcεRIα is shown in orange for illustration purpose by superimposing the full-length IgE model with the bound IgE^{Fc}/FcεRIα complex structure (PDB: 2Y7Q).

ARTICLE IN PRESS

TABLE E1. Three independent measurement sets of binding kinetics of FcεRIα to IgE variants

	Pertuzumab VH1-IgE			Pertuzumab VH2-IgE			Pertuzumab VH3-IgE			Pertuzumab VH4-IgE			Pertuzumab VH5-IgE			Pertuzumab VH6-IgE			Pertuzumab VH7-IgE		
	KD 10^{-10} (mol/L)	ka 10^{5} (1/Ms)	kd 10^{-5} (1/s)	KD 10^{-10} (mol/L)	ka 10^{5} (1/Ms)	kd 10^{-5} (1/s)	KD 10^{-10} (mol/L)	ka 10^{5} (1/Ms)	kd 10^{-5} (1/s)	KD 10^{-10} (mol/L)	ka 10^{5} (1/Ms)	kd 10^{-5} (1/s)	KD 10^{-10} (mol/L)	ka 10^{5} (1/Ms)	kd 10^{-5} (1/s)	KD 10^{-10} (mol/L)	ka 10^{5} (1/Ms)	kd 10^{-5} (1/s)	KD 10^{-10} (mol/L)	ka 10^{5} (1/Ms)	kd 10^{-5} (1/s)
Rep 1	4.33	2.10	0.91	6.67	1.42	9.49	2.55	2.21	5.65	2.21	2.36	5.19	0.42	1.90	0.80	4.08	1.70	6.94	5.52	1.39	7.66
Rep 2	5.06	2.02	1.02	5.46	1.55	8.46	3.18	2.23	7.08	1.59	3.85	6.11	0.09	2.23	0.21	5.75	1.35	7.74	2.35	2.60	6.11
Rep 3	4.91	2.52	1.24	5.22	2.13	11.2	2.60	2.81	7.31	4.92	2.01	9.89	0.66	1.63	1.07	10.6	1.13	12.1	3.58	2.56	9.17
Average	4.77	2.21	1.06	5.78	1.70	9.72	**2.78**	**2.42**	**6.68**	2.91	2.74	7.06	0.39	1.92	0.69	6.81	1.39	8.93	3.82	2.18	7.65

The boldface values are the reference values from Pertuzumab VH3-IgE. The underlined values highlight the variants VH5 and VH4 for comparison which are of interest to compare to the reference (VH3). *Ms*, Molarity × second.